Fusion of Airborne LiDAR and WorldView-2 MS Data for Classification of Depth to Permafrost within Canada's Sub-Arctic

L. Chasmer[1], C. Hopkinson[2], H. Morrison[2], R. Petrone[1], & W. Quinton[1]

[1]Cold Regions Research Centre, Wilfrid Laurier University, Waterloo ON N2L 3C5
lechasme@yahoo.ca
[2]Applied Geomatics Research Group, NSCC, Lawrencetown NS B0S 1M0

Abstract

The discontinuous permafrost zone of north-western Canada is characterised by a heterogeneous landscape of tree-covered permafrost plateaus that rise 0.5 m to 2.0 m above the surrounding fens and bogs. The depth to permafrost or "frost table" is influenced to some extent by vegetation canopy cover, which drives complex feedbacks related to permafrost thaw. Spectral remote sensing offers the possibility of large area mapping of canopy and ground surface characteristics that may be used as a proxy for permafrost thaw within remote northern areas. However, this depends on whether or not spectral bands can be used to identify slight variations in vegetation characteristics. The following study compares vegetation and topographic characteristics obtained using airborne Light Detection And Ranging (LiDAR) with high spatial resolution WorldView-2 spectral bands and *in situ* transect measurements of the depth to frost table. The results of this study indicate that the depth to the frost table is related to above ground vegetation cover and tree height, yet relationships are complicated by canopy and understory characteristics, topographic derivatives, and the position of the measured frost-table transect within the fragmented plateau. Comparisons between vegetation structural characteristics and WorldView-2 spectral bands are also examined so that confidence can be applied to depth of frost table estimates from WorldView-2 based on canopy characteristics. Discrete WorldView-2 pixels are related to depth to frost table (bands red, near infrared 1,2) and canopy metrics/topography obtained from airborne LiDAR. Variability is due, in part to absorption of near infrared by shadow fractions observed within WorldView-2 pixels, and spectral reflectance of ground vegetation visible within mixed pixels. High resolution spectral imagery, therefore, provides a link to processes controlling spatial variability of the depth to frost table.

Key Words: permafrost, discontinuous permafrost zone, multi-spectral remote sensing, WorldView-2, airborne LiDAR, vegetation structure.

1. Introduction

The southern boundary of discontinuous permafrost found in north-western Canada is highly sensitive to increases in air temperature via global warming in this region. Several studies have shown unprecedented permafrost thaw and the conversion of permafrost plateaus into bog and fen land cover types using historical aerial photography (e.g. Shur and Jorgenson, 2007; Quinton *et al.* 2010; Chasmer *et al.* 2010, 2011a). The conversion of plateaus into permafrost-free peatlands (ombrotrophic flat bogs and channel fens) strongly affects the hydrological nature of the watershed. Permafrost controls water storage and drainage processes by obstructing and re-directing the movement of water through channel fens and bogs (Quinton *et al.* 2010). The depth to permafrost, herein referred to as the "frost table", is influenced to some extent by radiation loading (Tarnocai *et al.*, 2004; Chasmer *et al.* 2011a), whereby up to 40% of the variance in frost table depth can be explained by the variation in canopy openness (Hopkinson *et al. in review*). Localised increases in shortwave radiation cause preferential thaw

of the active (or seasonally thawed) layer, which may result in a depression within the permafrost. Water drains towards the depression, resulting in a local increase in soil moisture and thermal conductivity (Hayashi *et al.* 2007).

Spatial variability of the existence of and depth to the plateau frost table has important implications for northern development and resources extraction, hydrology, and carbon and methane cycles. Given that permafrost underlies approximately 50% of the Canadian landmass, and that peatlands, which characterise a large proportion of northern ecosystems, contain approximately 1/3 of the global soil C pool (Gorham, 1991), large area mapping and assessment of proxies of permafrost change (e.g. plateau forest cover) is important. The following study examines relationships between the depth to frost table, vegetation and topographical characteristics measured using airborne Light Detection And Ranging (LiDAR), and spectral bands obtained from high spatial resolution WorldView-2 imagery across a permafrost plateau located within a typical watershed found in the Canadian discontinuous permafrost zone. The results of this study have implications for scaling and assessment of permafrost dynamics over broader areas using lower resolution multi-spectral satellite imagery.

2. Methods

2.1 Study area

The site is located approximately 50 kms south of Fort Simpson, within the Scotty Creek watershed (61° 18'N, 121° 18'W), Northwest Territories, Canada (Figure 1). The watershed is typical of the continental high boreal discontinuous permafrost/peatland region (National Wetlands Working Group, 1997). A supervised classification of IKONOS imagery (2000) (Quinton, *et al.* 2003) showed that approximately 43% of the watershed consisted of permafrost plateaus, ombrotrophic flat bogs (24%), channel fens (21%), lakes (9%), and isolated bogs (4%). Plateau extents are diminishing at an alarming rate (14% aerial reduction since 1970); with 73% of that area converting into bog as opposed to fen land cover types (Quinton *et al.* 2010; Kenward *et al. in review*). Permafrost plateaus support *Picea mariana* Mill. (black spruce) and a variety of shrubs and lichens. The mean annual temperature measured at Fort Simpson is -3^{o}C, while mean annual precipitation is 369 mm (1971 to 2000).

The depth to frost table was measured on August 2nd, 2010 along four ground-survey transects traversing north to south (one transect) and east to west (three transects) across a typical permafrost plateau (Figure 1). Depth to frost table was measured using a graduated steal measurement rod. The rod was pushed into the peat until it encountered frozen ground and could not be pushed in any further. Markings on the rod were used to determine the depth to frost table. Every measurement of frost table depth was geographically located using survey-grade differential GPS measurements (> 10 cm accuracy).

2.2 LiDAR data collection and processing

Airborne LiDAR data were collected by the authors (Applied Geomatics Research Group) for the entire Scotty Creek watershed on August 2nd, 2010 using an Optech Inc. ALTM 3100 four-pulse return system. The survey was parameterised for an averaging flying height of 1500 m a.g.l., with 50 kHz pulse repetition frequency, and a scan angle of ±20^{o}. Returns were classified into ground and non-ground (vegetation) within TerraScan software (Terrasolid, Finland) (Axelsson, 2000). Ground returns were used to create a 2 m resolution digital elevation model (DEM) using an inverse distance weighting approach. A digital surface model (DSM) was created based on the maximum laser pulse return (localised maxima) within a 2 m search radius. Canopy height was determined by subtracting the DSM from the DEM. Finally, gap

fraction was estimated as the ratio of the sum of all laser pulse returns between -1 m and + 0.5 m of the ground surface divided by the sum of all returns within a 1 m search radius.

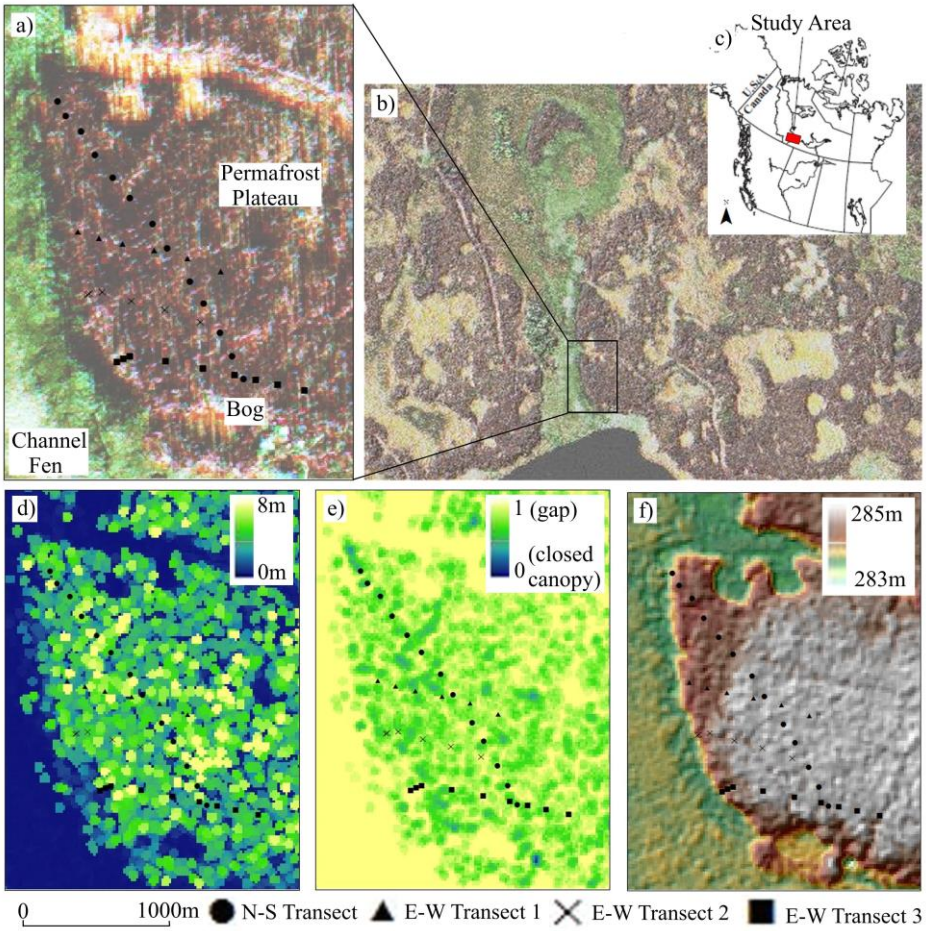

Figure 1: Depth to frost table measurement locations along four transects traversing the western edge of a permafrost plateau displayed as: a) WorldView-2 pan sharpened false colour composite of permafrost plateau, where red channel is WorldView band 6 (red edge), green channel is band 5 (red), and blue channel is band 3 (green); b) sub-area of watershed with LiDAR and WorldView-2 data collections. False colour composite in 'a' shown. Green areas = highly productive fen, red areas = treed permafrost plateaus, yellow = less productive bog; c) location of the study site in the Northwest Territories, Canada; LiDAR derived: d) canopy height model; e) gap fraction model; f) digital elevation model.

2.3 WorldView-2 image collection and orthorectification

Space-borne WorldView-2 (DigitalGlobe Corp.) was tasked for imaging of the Scotty Creek watershed between September 17 and October 1, 2010 (resulting in two cloud-free images) via MDA Corp. Canada. WorldView-2 data were obtained as a standard, radiometrically corrected ortho-ready bundle including a 0.65 m panchromatic image (400-900 nm) and eight narrow spectral bands: coastal (400-450 nm), blue (450-510 nm), green (510-580 nm), yellow (585-625 nm), red (630-690 nm), red edge (705-745 nm), near infrared 1 (NIR1, 770-895 nm), and near infrared 2 (NIR2, 860-1040 nm) at 2 m pixel resolution. The look angle was 20^{o} maximum off nadir. Data were processed to UTM coordinates matching that of the LiDAR data (NAD83 CSRS). The watershed was divided into 2 km x 2 km tiles and imported into Geomatica OrthoEngine (PCI Inc. Canada) using the WorldView-2 mosaic and colour-balancing tool. The colour-balanced, mosaiced imagery was then orthorectified using the LiDAR DEM, 2 m

resolution gridded ground surface laser return intensity and 23 tie points located within both datasets at the intersections of trails and seismic lines. The images were orthorectified to better than 1 m accuracy using a second order polynomial transformation in OrthoEngine. Table 2 provides summary statistics of WorldView-2 spectra per band along transects. Pixel digital numbers (DN) were then converted to top-of-atmosphere spectral radiance (Wm^{-2} sr^{-1} μm^{-1}) based on absolute radiometric calibration factors (Wm^{-2} sr^{-1} $count^{-1}$) provided per band to get a band-integrated radiance (Wm^{-2} sr^{-1}). This is then divided by effective bandwidth to get spectral radiance.

2.3 Statistical analysis

LiDAR vegetation (CHM, gap fraction) and elevation (DEM) metrics, and WorldView-2 spectral bands were compared with depth to frost table measurements within 1 m and 2 m radii of the measurement location (pixel/cell averages, maximum, minimum, and standard deviations presented) (Morrison, et al. *this issue of SilviLaser*). Only depth to frost table measurements located on the plateau (as opposed to plateau edges) are described. Processes associated with permafrost thaw at the edge of plateaus can differ from those within plateaus, and therefore, measurements at the edge of plateaus were excluded from this analysis. (A more comprehensive assessment of the LiDAR and frost table depth spatial correlations is presented in Hopkinson *et al*. *in review*). The numbers of measurements included along transects were: 13 (N-S transect), 6 (E-W transect 1), 6 (E-W transect 2) and 9 (E-W transect 3) for a total of 34 measurements. Comparisons were made using linear and non-linear (where required) regression and tests of significance.

3. Results and Discussion

3.1 General observations along transects

The results of this study provide some promise as to the use of WorldView-2 spectral imagery for detecting i) areas underlain by permafrost; and ii) the relative depth to permafrost as a function of canopy cover. In many cases, airborne LiDAR data may not be needed. This could extend the application of this study to other remote northern environments not surveyed by LiDAR.

Measurements along transects that have tallest trees, fewer within canopy gaps, and slightly upraised elevation are characterised by frost table depths not far below the ground surface (on average) (Table 1, characteristic transects in *italics*). Along one transect, however (E-W Transect 3), close proximity to the southern edge of the plateau, shorter trees, and greater within canopy gaps may have contributed to increased thaw down of the frost table. This is especially evident along parts of the transect that traversed the plateau near an area of plateau collapse and an overland flow channel (Table 1, normal text).

Table 1: Depth to frost table, vegetation and ground surface elevation summary statistics (average and standard deviation (σ)) for transects. Statistics are based on LiDAR metric extractions within 1m of frost table depth measurement locations.

Transect	Average (σ) depth to frost table (m)	Average (σ) canopy height (m)	Average (σ) gap fraction	Average (σ) elevation (m)
N-S Transect	*-0.47 (0.08)*	*4.9 (0.9)*	*0.75 (0.11)*	*284.5 (0.32)*
E-W Transect 1	*-0.52 (0.07)*	*5.0 (1.3)*	*0.81 (0.10)*	*284.6 (0.32)*
E-W Transect 2	*-0.50 (0.06)*	*4.5 (0.95)*	*0.79 (0.10)*	*284.5 (0.40)*
E-W Transect 3	-0.56 (0.09)	3.2 (1.5)	0.87 (0.12)	284.5 (0.30)

Comparisons of average (and σ) band radiance between transects illustrate some variability associated with canopy, understory and ground surface characteristics. Optically bright reindeer lichen (*Cladina mitis; Cladina rangiferina*), and senescing short deciduous shrubs (*Oxycoccus microcarpus; Ledum groenlandicum*) found along Transects 1 and 3 (E-W) have contributed to increased reflectance in green, red edge, NIR1 and NIR2 bands. Reduced spacing between trees and increased within canopy shadows along transects N-S and E-W 2 may have resulted in reduced reflectance in NIR1 and 2 bands. Are variations in spectral radiance a proxy indicator of frost table depth between transects?

Table 2: WorldView-2 spectral radiance (Wm^{-2} sr^{-1} μm^{-1}) summary statistics within 1 m radius of depth to frost table measurements per transect.

Transect	Ave. (σ) WV2 B1 (coast)	Ave. (σ) WV2 B2 (blue)	Ave. (σ) WV2 B3 (green)	Ave. (σ) WV2 B4 (yellow)	Ave. (σ) WV2 B5 (red)	Ave. (σ) WV2 B6 (red edge)	Ave. (σ) WV2 B7 (NIR1)	Ave (σ) WV2 B8 (NIR2)
N-S	32.11	27.96	17.74	12.19	9.18	13.88	14.41	10.11
Transect	(6.31)	(3.75)	(1.59)	(1.66)	(1.26)	(1.60)	(1.27)	(0.92)
E-W	32.30	28.18	9.17	13.12	9.46	15.65	16.30	12.25
Transect 1	(6.35)	(3.78)	(0.82)	(1.79)	(1.30)	(1.81)	(1.44)	(1.11)
E-W	32.09	27.66	17.35	12.29	8.95	13.65	13.50	11.10
Transect 2	(6.31)	(3.71)	(1.56)	(1.68)	(1.23)	(1.58)	(1.19)	(1.01)
E-W	32.64	28.62	18.66	13.57	10.41	16.62	16.38	12.61
Transect 3	(6.41)	(3.84)	(1.67)	(1.85)	(1.43)	(1.92)	(1.45)	(1.14)

3.2 Correspondence between WorldView-2 bands and variability in frost table depth

Variability in frost table depth across all transects did not correspond well with radiance from WorldView-2 spectral bands. At best, increased reflectance in red wavelengths corresponds significantly, but not strongly with increased depth to permafrost (r^2 = 0.09, p <0.001, RMSE =0.07 m for red band). Thus, WorldView-2 spectral radiance is confounded by within and below canopy averaging within pixels and variability when examined across transects. Mixed pixels caused by narrow black spruce canopies and leaning trees (as permafrost thaws), poorly drained and dry upraised peat soils, and groups of shrubs and reindeer lichen alter within pixel spectral reflectance. The location of transects on the plateau surface, and feedbacks between soil moisture (at the edge of plateaus), and fragmentation also confound relationships. Yet, within transects, some interesting relationships between vegetation/ground surface structure, spectral reflectance, and depth to frost table can be found.

3.3 Comparisons between airborne LiDAR metrics and WorldView-2 along transects

Within transects, airborne LiDAR metrics of canopy height, elevation, and to a lesser extent gap fraction correspond significantly with WorldView-2 spectral bands. However, coefficients of variation (r^2) often explain up to only one third of the variability, indicating some complexity remains unexplained:

1. Mean canopy heights within 2 m of individual frost table depth measurements are negatively related to mean reflectance in the red band (r^2 = 0.34, p < 0.001, RMSE = 1.44 m). Red reflectance decreases with greater pixel fractions containing trees (often positively related to canopy cover (r^2=0.19).
2. Variability of maximum canopy gaps within 1 m radius of frost table depth measurements are positively related to increased variability in NIR2 band (r^2 = 0.21, p <0.001, RMSE = 9%) due to reduced within canopy shadowing.
3. Variations in elevation within a 2 m radius of frost table depth measurements are

explained by between pixel standard deviation in the red band, where increased variability often results in increased red reflectance ($r^2 = 0.21$, $p < 0.001$, RMSE = 0.09 m).

Within individual transects, spectral radiance may be used to estimate variability in the depth to frost table, depending on vegetation and ground surface characteristics defined by LiDAR. Taller trees found along N-S Transect are associated with increased reflectance in the green band ($r^2 = 0.52$, $p < 0.01$), increased ground surface shadowing, and reduced depth to frost table (Table 3). Along E-W Transect 1, green reflectance from the ground, as opposed to that from widely spaced trees may be linked to increased tree bole illumination and sensible heat inputs from tree boles into the ground surface (thereby increasing permafrost thaw; Chasmer *et al.* 2011; Hopkinson *et al. in review*). Similar results were also found along E-W Transect 2, which was characterised by some ground surface shadowing and absorption in NIR bands. Spectral reflectance within red edge wavelengths was indicative of senescing black spruce trees, successive deciduous shrub development, and tall grasses often found at waterlogged plateau edges and within areas of plateau slump (Table 3).

Table 3: Strongest relationships between depth to frost table and WorldView-2 bands within transects.

Transect	WorldView band	r^2 (p)	RMSE (m)	Distance from depth to frost table measurement
N-S Transect	Green	0.18 (0.008)	0.06	1 m, minimum radiance
E-W Transect 1	Green	0.94 (<0.001)	0.02	1m, minimum radiance
E-W Transect 2	NIR2	0.81 (<0.001)	0.03	2m, minimum radiance
E-W Transect 3	Red Edge	0.71(<0.001)	0.05	2m, σ

4. Conclusions

This study compares measurements of the depth to frost table with high resolution multispectral WorldView-2 imagery and vegetation structural/topographic metrics derived from airborne LiDAR data. The purpose was to determine if structural/topographic metrics that influence the spatial variability of the depth to frost table can be examined using spectral remote sensing imagery at the end of the growing season. This study has shown that variability in depth of frost table can be estimated using green and NIR bands, however, the strength of the relationships vary with spatial variability of local canopy height, spacing between vegetation, shadows, and proximity to plateau edge (within up to 2 m from the frost table depth measurement). WorldView-2 spectral bands, red and NIR2 can also be used to estimate canopy height, canopy gaps, and elevation.

Acknowledgements

Funding for this project was provided by an NSERC Strategic Grant provided to Dr. Quinton, and a CFI grant provided to the AGRG LiDAR Laboratory for purchase of the airborne LiDAR and infrastructure. Thank-you also to Tristan Goulden, and Allyson Fox for assistance with LiDAR data collection, processing, and field work. Also thanks to the Liidlii Kue First Nation.

References

Axelsson, P., 2000, DEM generation from laser scanner data using adaptive TIN models, *IAPRS 2000*, 33(B4), 110-117.

Chasmer, L., Hopkinson, C. and Quinton, W., 2010, Quantifying errors in discontinuous permafrost plateau change from optical data, Northwest Territories, Canada: 1947 to 2008. *Canadian Journal of Remote Sensing*, 36(2):S211-S223.

Chasmer, L., Quinton, W., C. Hopkinson, R. Petrone, and P. Wittington, 2011a, Vegetation canopy and radiation controls on permafrost plateau evolution within the discontinuous permafrost zone, Northwest Territories, Canada, *Permafrost and Periglacial Processes*, DOI: 10.1002/ppp.724.

Chasmer, L., Kljun, N., Hopkinson, C., Brown, S., Milne, T., Giroux, K., Barr, A., Devito, K., Creed, I., and Petrone, R. 2011b. Characterizing vegetation structural and topographic characteristics sampled by eddy covariance within two mature aspen stands using LiDAR and a flux footprint model: Scaling to MODIS. *Journal of Geophysical Research-Biogeosciences, Special Issue on Advances in Upscaling of Eddy Covariance Measurements of Carbon and Water Fluxes, 115*, doi:10.1029/2010JG001567.

Gorham, E. 1991, Northern Peatlands: Role in the Carbon-Cycle and Probable Responses to Climatic Warming, *Ecological Applications,* 1(2),182-195.

Hopkinson, C., Chasmer, L., W. Quinton, Assessing spatial coincidence between forest canopy and discontinuous permafrost features using LiDAR and thermal image data, *Hydrological Processes (in review)*.

Hayashi, M., Goeller, N., Quinton, W., and Wright, N., 2007, A simple heat-conduction method for simulating the frost-table depth in hydrological models. *Hydrological Processes*, 21,2610-2622.

Kenward, A., Chasmer, L., Petrone, R., and W. Quinton, Spatial and temporal variability of CO_2 exchanges along a fen-plateau-bog transect within the discontinuous permafrost zone, Northwest Territories: Implications for landscape change, *Ecosystems (in review).*

National Wetlands Working Group, 1997. The Canadian Wetland Classification System, 2nd Ed.

Quinton, W.L., Hayashi, M., and Pietroniro, A., 2003. Connectivity and storage functions of channel fens and flat bogs in northern basins. *Hydrological Processes*. 17,3665-3684.

Quinton, W., Hayashi, M., and Chasmer, L., 2010. Permafrost thaw in the Canadian sub-arctic: Some implications for water resources. *Hydrological Processess Scientific Briefing.* DOI: 10.1002/hyp.7894.

Shur, Y.L., and Jorgenson, M.T. 2007. Patterns of permafrost formation and degradation in relation to climate and ecosystems. *Permafrost and Periglacial Processes*. 18,7-19.

Tarnocai, C., Nixon, F.M. and Kutny, L. 2004. Circumpolar-Active-Layer-Monitoring (CALM) sites in the Mackenzie Valley, northwestern Canada. *Permafrost and Periglacial Processes*. 15,141-153.